Geometric control of robotic locomotion systems

Sonia Martínez[1] and Jorge Cortés[2]

[1]*Instituto de Matemáticas y Física Fundamental*
Consejo Superior de Investigaciones Científicas
Serrano 123, 28006 Madrid - Spain

[2]*Faculty of Mathematical Sciences*
University of Twente
PO Box 217, 7500 AE Enschede - The Netherlands

emails: s.martinez@imaff.cfmac.csic.es, j.cortesmonforte@math.utwente.nl

Abstract

A wide class of robotic locomotion systems share a rich unifying geometric framework where notions such as cyclic rectification, coupling and motions induced by the interaction with the environment have a proper mathematical formulation. In this paper, we show how the modeling of robotic systems based on Lagrangian reduction techniques enables us to approach the optimal control problem in a way where locomotion concepts are naturally introduced. We propose an algorithm to numerically solve this optimal control problem and explore its convergence properties. Finally, several simulations and comparisons with experimental motions are shown for the robotic eel mechanism REEL II.

Key words: Robotic locomotion systems, Geometric Mechanics, optimal control theory.
MSC 2000: 93B29, 70E60, 65Kxx

1   Introduction

In the recent decades, the field of robotics has experimented a spectacular growth and robots are nowadays common tools in different scenerios of industry, space exploration and medicine, to name a few. Due in part to their mythification by the entertainment industry, robots have enjoyed a great deal of popularity and social impact. Since they first appeared in Capek's play

Rossum's Universal Robot (R. U. R.), where human-like robots worked tirelessly to relieve their human creators from the hardest tasks, the idea of robots as tools with endless possibilities has excited our minds and given rise to a new technology of specialized machines.

A first classification of the many robots that there exist may be given on the basis of its mobility. *Fixed robots* constitute the major type of industrial robot that usually consists of a programmable arm with several degrees of freedom. These robots are capable of very complex tasks that may require high accuracy and velocity such as circuits or engine assembly, car welding and painting, or other tasks of the automotive industry.

On the other hand, *mobile robots* were designed with the aim of obtaining machines that could operate in unreachable or hazardous environments. For example, here we find the wide class of *autonomous vehicles* mainly employed in space and submarine exploration. These programmable vehicles include wheeled or tracked cars, underwater vehicles or aircrafts which are in some cases provided with robotic arms to carry out their tasks.

In searching for more efficient and robust solutions to problems of locomotion, roboticists have turned their attention to *biological* or *biomimetic robots.* The biomimetic approach uses biology as a model for the development of new systems, and has already inspired other branches of engineering such as computer vision and artificial intelligence. For example, an area which has been widely investigated is that of *walking.* Contrary to what happens with wheeled systems, walking or hopping robots would be better adapted to rough or uneven terrain, or even able to climb stairs and ladders. In this way, hexapods and other four and two-legged robots [11, 15] have been developed trying to reproduce walking *motion patterns* or *gaits.*

Along with wheeled mobile platforms and legged locomotion, other forms of robotic (and biological) locomotion that have been studied are related to the area of *swimming,* including snake-like motions [2, 7], inchworm motions [8], and even the motion of water-bugs and paramecia [6, 10, 17]. As opposed to underwater vehicles that rely on propellers or similar devices to move, fish-like swimmers propulse themselves by the vorticity produced in their tail that they deform. This makes fishes very agile and capable of high accelerations [14]. Finally, in the area of flapping mode *flying* systems, there have been some recent advances [18], though the problem of stabilizing a flapping system presents an additional difficulty.

A wide class of locomotion systems possess common features that allows a description within the same unifying geometric framework [8, 21]. This has made possible the general treatment of the *controllability analysis* and the *motion planning* problems for general locomotion systems. In this paper

we shall explore this topic reviewing some of the ideas developed in [19, 21]. In particular we will discuss extensively the optimal control problem for the REEL robot [3, 13, 16].

2   Modeling and Lagrangian reduction

When studying *locomotion systems* (see for instance [8, 21]), two fundamental characteristics appear to be common to a number of them. The first one, which accounts for the term locomotion, is that they involve *motion* from one place to another in $\mathbb{R}^2$ or $\mathbb{R}^3$. Usually, if the environment where the motion takes place is of an homogeneous nature, the system will exhibit rotational and/or translational symmetries. On the other hand, another common feature is observed in the way in which motion is achieved: a wide range of systems rely on the *cyclic rectification* of their shape and their *interaction* with the environment to effectively move.

As an example of this, consider a person walking on the floor. If the floor is more or less horizontal, this person will not change his/her way of walking independently of his/her position and orientation on the ground. In this way, (s)he will exhibit traslational and rotational symmetry. On the other hand, the person moves his/her legs cyclically and it is due to the friction forces between his/her feet with the ground that (s)he moves forward without slipping.

In view of this, one could employ the following ingredients in the modeling of locomotion systems,

- an n-dimensional manifold Q describing the set of all the possible configurations of the system,

- a Lagrangian function $L : TQ \longrightarrow \mathbb{R}$ which governs the dynamics of the system, and

- a differentiable distribution $\mathcal{D} : Q \longrightarrow TQ$ modeling certain constraints of kinematic type (1-forms of Pfaffian type) or interaction with the environment.

When examining many locomotion systems a natural splitting in the configuration space occurs, $q = (g, r) \in Q = G \times M$, where $g \in G$ stands for the position (and orientation) of the body, and $r \in M$ denotes the internal *shape* of the system (see example below). We will refer to G as *the pose space* (from position and orientation) and M as *shape space*, following standard terminology in locomotion [3, 8, 13, 16, 19].

In this way Q becomes a *trivial principal fiber bundle* [9] with base space M and fiber space G. Denote by $\Phi : G \times Q \to Q$ the action of G on Q and

$\pi : Q \to M$ the projection of Q onto M. The sets $\mathrm{Orb}_G(q) = \{\Phi(g, q) \,|\, g \in G\}$ become the vertical fibers of π and the spaces $T_q\mathrm{Orb}_G(q) \equiv V_qQ \leq T_qQ$ define the vertical subbundle VQ of TQ.

Since the system will exhibit symmetry with respect to the Lie group, L and $\mathcal{D}$ are to be compatible with the structure of Q as follows,

$$L(\Phi_g(q), T_q\Phi_g(\dot{q})) = L(q, \dot{q}), \qquad T_q\Phi_g(\mathcal{D}_q) \subseteq \mathcal{D}_{\Phi_g(q)}.$$

The equations of motion of the system can now be written with the help of a *principal connection A*, which takes into account the symmetry properties of the system. A principal connection $A : TQ \longrightarrow \mathfrak{g}$ provides a G-invariant horizontal subbundle complementary to VQ in TQ. That is,

$$H_qQ = \{v_q \in T_qQ \,|\, A(q)v_q = 0\}, \qquad H_qQ \oplus V_qQ = T_qQ, \quad \forall q \in Q.$$

A is given in different ways depending on the type system under consideration. For example, the *mechanical connection* [22] is used for modeling unconstrained systems. In this case, the equations of motion may be written as

$$\xi = g^{-1}\dot{g} = -\mathsf{A}(r)\dot{r} + I^{-1}(r)p,$$
$$\dot{p} = ad_\xi^* p,$$
$$M(r)\ddot{r} = -C(r, \dot{r}) + N(r, \dot{r}, p) + \tau_r.$$

Here $ad^* : \mathfrak{g} \times \mathfrak{g}^* \to \mathfrak{g}^*$ is the dual map of the adjoint action of the Lie algebra onto itseft, $\mathsf{A}(r)$ is called the "local form" of the mechanical connection and I is the locked inertia tensor [1, 19]. $I(r)$ describes the total inertia of the system when the shape is frozen at r.

The *nonholonomic connection* [1] is used for modeling constrained systems. This situation is richer and the connection's definition depends upon the compatibility of constraints and symmetries, described by the intersection $\mathcal{D} \cap VQ$.

- The *kinematic case* corresponds to $\mathcal{D} \cap VQ = 0$. In this case the equations describing the system are simply

$$\xi = g^{-1}\dot{g} = -\mathsf{A}(r)\dot{r},$$
$$M(r)\ddot{r} = -C(r, \dot{r}) + \tau_r.$$

Observe that we can rewrite the second equation as $\ddot{r} = u$, if we assume total control of the shape by applying appropriate torques τ_r. Integrating this equation once, we can reduce the system to a first order or *kinematic* system.

- The *mixed (dynamic) case* occurs when $\mathcal{D} \cap VQ \neq 0$. The equations of motion include now the *nonholonomic momentum equation*, which makes the system *dynamic*,

$$g^{-1}\dot{g} = -\mathcal{A}(r)\dot{r} + \mathcal{I}^{-1}(r)p \,,$$
$$\dot{p} = \frac{1}{2}\dot{r}^T\sigma_{\dot{r}\dot{r}}(r)\dot{r} + p^T\sigma_{p\dot{r}}(r)\dot{r} + \frac{1}{2}p^T\sigma_{pp}(r)p \,,$$
$$M(r)\ddot{r} = -C(r,\dot{r}) + N(r,\dot{r},p) + \tau_r \,.$$

Observe that in all the above-exposed systems, the local form of the connection determines the system's motion in G and Q as a combination of the momentum, p, and the internal shape changes $(r, \dot{r})$, which are actuated through the torques τ_r. Closed curves or *gaits* in the shape space M couple with the environment through the principal connection to induce motions in the pose space G. Thus, the principal connection is precisely the geometric object that synthesizes the process of locomotion. This fact has been found to be very useful for control analysis purposes and even as an instrument to tackle motion planning problems [8, 19, 20].

3   The robotic eel REEL II

The eel robot of Figure 1 is an example of underactuated robotic locomotion system. It was studied in [16] to test various locomotive gaits. The robotic eel gets to move in a wet environment by effecting a traveling wave down its body by means of torques applied at its joints. The dynamic effects of the robot are not negligible and thus the motion planning problem (MPP) for the eel is not trivial. Usually, the MPP is decoupled into two phases. First, in a *low level*

Figure 1: The REEL II robot manufactured in the GRASP lab.

problem, a path in Q is generated mainly using techniques from computational

geometry. And after that, in a *high level problem*, feedback control laws are designed so that the system tracks the trajectory obtained in the low level problem. A first inconvenience of this method is that the dynamics of the real system is not taken into account. The robot may not move in arbitrary directions and the method could give rise to non-differentiable solutions which are very costly to implement in the real system. In this regard, the new approach employed with the REEL in [16] tries to solve the MPP in a single step, taking into account the real dynamics.

The model of the REEL (see Figure 2) consist of a planar, serial chain of 5 identical links of length $2d$, mass m and inertia J, and each joint is assumed to be independently actuated. All of the eel possible configurations
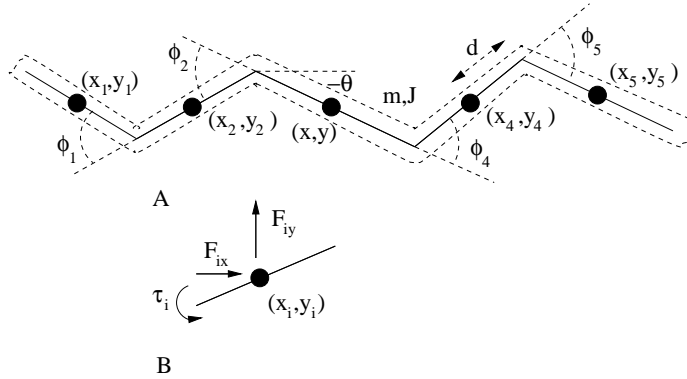
Figure 2: A. Model of the eel as a planar, serial chain of links. B. Forces and torques on link i.

are determined by $(x, y, \theta) \in SE(2)$, giving the position and orientation of the middle link, and $(\phi_1, \phi_2, \phi_4, \phi_5) \in \mathbb{S}^1 \times \mathbb{S}^1 \times \mathbb{S}^1 \times \mathbb{S}^1$, denoting the angles of each joint. Thus, the configuration space becomes $Q = SE(2) \times \mathbb{S}^1 \times \mathbb{S}^1 \times \mathbb{S}^1 \times \mathbb{S}^1$. The G-invariant Lagrangian of the system is defined as the kinetic energy

$$L = \frac{1}{2}m(\dot{x}^2 + \dot{y}^2) + \frac{1}{2}J\dot{\theta}^2 + \frac{1}{2}J\sum_{i \neq 3}\left(\sum_{j=h(i)}^{i}\dot{\phi}_j + \dot{\theta}\right)^2 + \frac{1}{2}m\sum_{i \neq 3}\left(\dot{x}_i^2 + \dot{y}_i^2\right),$$

by means of (x_i, y_i), the coordinates of the center of the ith link, which can be

specified as

$$\begin{pmatrix} x_i \\ y_i \end{pmatrix} = \begin{pmatrix} x \\ y \end{pmatrix} + sg(i)d \begin{pmatrix} \cos\theta \\ \sin\theta \end{pmatrix}$$

$$+ sg(i)d \sum_{k=h(i)}^{i} f(i,k) \begin{pmatrix} \cos(\theta + \sum_{j=h(i)}^{k} \phi_j) \\ \sin(\theta + \sum_{j=h(i)}^{k} \phi_j) \end{pmatrix},$$

where

$$sg(i) = \begin{cases} -1 & \text{if } i < 3 \\ 1 & \text{if } i > 3 \end{cases} \qquad f(i,k) = \begin{cases} 2 & \text{if } i \neq k \\ 1 & \text{if } i = k \end{cases} \qquad h(i) = \begin{cases} 2 & \text{if } i < 3 \\ 4 & \text{if } i > 3 \end{cases}$$

The interaction of the robot with the environment will be modeled by frictional forces. By taking different expressions for these, we can model different types of locomotion systems such as the eel in water or on dry land. Based on previous work [4], the following expression for the drag forces were taken in [16]. Approximately,

$$|F_i| \approx \mu_w v_i^2$$

opposing the velocity v_i and it was assumed that pressure differentials in the directions parallel to the moving body decoupled from pressure differentials perpendicular to the body. This yields

$$F_i^{\parallel} = -\mu_w^{\parallel} \text{sgn}(v_i^{\parallel}) \cdot (v_i^{\parallel})^2, \qquad F_i^{\perp} = -\mu_w^{\perp} \text{sgn}(v_i^{\perp}) \cdot (v_i^{\perp})^2, \tag{1}$$

where $\mu_w^{\parallel}$ and $\mu_w^{\perp}$ are drag coefficients for the water and $v_i^{\parallel}$, $v_i^{\perp}$ are the projections of the vector $(\dot{x}_i, \dot{y}_i)$ along the direction parallel and perpendicular to the link, respectively. For the purposes of simulation, we will limit our attention to a linear, viscous force approximation of the form,

$$F_i^{\parallel} = -\mu_v^{\parallel} v_i^{\parallel}, \qquad F_i^{\perp} = -\mu_v^{\perp} v_i^{\perp},$$

where $\mu_v^{\parallel}$, $\mu_v^{\perp}$ are coefficients of viscous drag. This can be thought of as a first-order approximation to the quadratic drag forces described in equation (1), which we note are also odd functions of the velocity. In general, for systems with periodic behavior, viscous forces approximations can be used, provided coefficients of friction are chosen to dissipate an equal amount of energy over one cycle of motion. Frictional forces are G-invariant. We denote

$$\tau^{\parallel}(r,\dot{r},\xi) = F^{\parallel}(r,g^{-1}g,\dot{r},g^{-1}\dot{g}), \qquad \tau^{\perp}(r,\dot{r},\xi) = F^{\perp}(r,g^{-1}g,\dot{r},g^{-1}\dot{g}).$$

With this in mind the derivation of the expression for the frictional foces for the eel is straighforward though not trivial. We refer to [3] for the explicit expression of these as well as of the equations of motion.

Now, following a Lagrangian reduction procedure as described before we can obtain the equations of motion for the eel as

$$g^{-1}\dot{g} = -\mathsf{A}(r)\dot{r} + I^{-1}(r)p\,,$$

$$\dot{p} = p^T \sigma_{p\dot{r}}(r)\dot{r} + \frac{1}{2}p^T \sigma_{pp}(r)p + \tau(r,\dot{r},\xi)\,, \qquad (2)$$

$$M(r)\ddot{r} = -C(r,\dot{r}) + N(r,\dot{r},p) + \tau_r = M(r)w\,,$$

$$\Longleftrightarrow \ddot{r} = w \Longrightarrow \dot{r} = u\,,$$

where τ_r corresponds to the torques that act internally and τ are the drag forces of the environment. The connection that is being used here is the mechanical connection. Observe that we are assuming full control of the shape variables $u_i = \dot{\phi}_i$, which is reasonable, since the eel robot has actuators at each joint.

Observe that equations (2) can be put into the standard form of an affine-input nonlinear control system

$$\dot{z} = f(z) + B(z)u\,,$$

where the states are $z = (g,p,r) \in G \times \mathbb{R}^s \times M$, the non-zero drift is

$$f(z) = \begin{pmatrix} g\,I^{-1}(r)p \\ \frac{1}{2}p^T \sigma_{pp}(r)p + \rho_p(r)p \\ 0 \end{pmatrix}\,,$$

and $B = (B_i(z))$, the control matrix, becomes

$$B_i(z) = \begin{pmatrix} -gA(r)e_i \\ (p^T \sigma_{p\dot{r}}(r) + \rho_{\dot{r}}(r))e_i \\ e_i \end{pmatrix}\,, \quad 1 \le i \le \dim(M) = m\,.$$

Here e_i denotes an m-vector having a 1 in the ith row and 0 otherwise. The input vector $u(t) \in \mathbb{R}^m$ is defined to be $u_i(t) = \bar{w}_i(t)$, where

$$\bar{w}_i(t) \equiv \int_0^t w_i(s)ds\,, \quad w = \ddot{r}\,,$$

that is, u is a velocity input.

4   The optimal control problem: Basis Algorithm

In [16], the equations of the eel in the form of (2) were used to solve the motion planning problem for the REEL by means of a perturbative approach. It was

found that the eel was a controllable system by showing how different gaits gave rise to forward, turning-in-place and parallel motions. The next question that seems natural to be addressed is how to choose the input functions in a way that is *optimal* with regards to some criterion. That is, we are interested in solving the following *optimal control problem*,

---

OCP1: *Given z_0, z_f, determine $u \in \mathcal{U}$ such that the solution of*

$$\begin{cases} \dot{z} = f(z) + B(z)u \\ z(0) = z_0 \end{cases} \qquad \textit{satisfies } z(T) = z_f \,,$$

after time $T > 0$ while minimizing the cost functional

$$\mathcal{J}(u) = \int_0^T \left(u_1(t)^2 + \cdots + u_m(t)^2 \right) dt \,.$$

Here,

$$\mathcal{U} = \left\{ u : [0,T] \longrightarrow \mathbb{R}^m \,\middle|\, \begin{array}{c} u(t) \text{ is piecewise differentiable and} \\ u(0) = u(T) \; T\text{-periodic} \end{array} \right\} \,,$$

corresponding to the fact that we search for closed curves (gaits) in the shape space M.

In trying to solve this problem for driftless systems a numerical approach was taken in [5] based on the following observation. Note that $\mathcal{U} \subset L_2[0,T]$ and $\mathcal{J}(u) \triangleq \|u\|_{L_2}^2$. Taking $\{\mathbf{e}_i(t)\}_{i=1}^{\infty}$ an orthonormal basis for $L_2[0,T]$, we can write $u(t) = \sum_{i=1}^{\infty} \alpha_i \mathbf{e}_i(t)$ for some $\alpha = (\alpha_i)_{i=1}^{\infty} \in l_2$ and then the OCP1 can be rephrased as an infinite dimensional problem in l_2,

---

OCP2: *Given z_0 and z_f, determine $\alpha \in l_2$ find of minimum cost,* $\mathcal{J}(\alpha) = \sum_{i=1}^{\infty} \alpha_i^2 \triangleq \|\alpha\|_{l_2}^2$, *such that the solution*

$$\begin{cases} \dot{z} = f(z) + B(z)(\sum_{i=1}^{\infty} \alpha_i \mathbf{e}_i(t)) \\ z(0) = z_0 \end{cases} \qquad \textit{satisfies } z(T) = z_f \,.$$

Finding an analytical solution of the OCP1 or the infinite-dimensional OCP2 turns out to be very difficult in general. One possible idea to overcome this problem is approximate numerically the solutions of OCP2 that arise from the truncation of the series to the first basis elements. That is, by restricting the set of inputs to

$$\mathcal{U}_N = \left\{ u \in \mathcal{U} \,\middle|\, u(t) = \sum_{i=1}^{N} \alpha_i \mathbf{e}_i(t) \,, \alpha = (\alpha_1, \ldots, \alpha_N) \in \mathbb{R}^N \right\} \,,$$

for some $N > 0$. In this way, we will look for *sub-optimal* solutions or *near-optimal* gaits. Based on previous work [5, 21], it is reasonable to choose $\{\sin(nt), \cos(nt)\}_{n=1}^{\infty}$ for treating undulatory locomotion systems with non-zero drift. The issue of whether the system is still controllable using this truncated basis is a subtle one. However, it has been shown that undulatory locomotion systems [12, 19] such as the eel system, are locally controllable using such a class of inputs. In the following, we discuss the basis algorithm developed in [5], which was adapted in [3] to control systems with non-zero drift. For the technical aspects and a more detailed exposition we refer the reader to [3].

Basis Algorithm

First, we take an $N \in \mathbb{N}$ and define $\Phi = (\mathbf{e}_1, \ldots, \mathbf{e}_N)$. Truncating the OCP2 to the first N basis elements we get

$$\begin{cases} \dot{z} = f(z) + B(z)\,\Phi\,\alpha^T \\ z(0) = z_0 \,. \end{cases} \tag{3}$$

A given $u \in \mathcal{U}_N$ or $\alpha = (\alpha_1, \ldots, \alpha_N) \in \mathbb{R}^N$ determines a solution $z(t, \alpha)$ of (3). Clearly, as $f(z)$ and $B(z)$ are taken to be smooth, $z(T, \alpha)$ will vary smoothly with α and so will do the function

$$\begin{aligned} g : \mathbb{R}^N &\longrightarrow \mathbb{R}^d \\ \alpha &\longmapsto z(T, \alpha) \,. \end{aligned}$$

Choose now a $\gamma \in \mathbb{R}_+$. Then, we approximate the OCP2 by the following finite-dimensional problems.

$P_{N,\gamma}$**:** *Given $N \in \mathbb{N}$ and $\gamma > 0$, determine the solutions $(z_{N,\gamma}^*, \alpha_{N,\gamma}^*)$ of (3) that minimize*

$$\mathcal{J}_{N,\gamma}(\alpha) = \langle \alpha, \alpha \rangle + \gamma \|g(\alpha) - z_f\|_{\mathbb{R}^d}^2 \triangleq \sum_{i=1}^{N} \alpha_i^2 + \gamma \|g(\alpha) - z_f\|_{\mathbb{R}^d}^2 \,.$$

Finally, we approximate the solutions of $P_{N,\gamma}$ numerically. This is done by obtaining a sequence $\{\alpha_k\}$ that eventually will tend to $\alpha_{N,\gamma}^*$. To do this, we used a modified Newton's rule [3].

Correctness of the Basis Algorithm

In [3] we proved that under the following assumption,

Bounded Input Bounded State stability: *There exists a continuous $\phi(\delta, z_0)$, $\delta \geq 0$ such that if $\|u\|_2 \leq \delta$ then the corresponding solution $z(t)$ verifies $\|z\|_{C[0,T]} = \sup_{t \in [0,T]} \|z(t)\|_{\mathbb{R}^d} \leq \phi(\delta) < \infty$,*

the solutions of $P_{N,\gamma}$ will tend to solutions of OCP2 as N, $\gamma \longrightarrow \infty$ in the following sense.

Theorem 4.1. *Let $S_* \subseteq C[0,T] \oplus L_2[0,T]$ be the set of optimal solutions (z_*, u_*) of the original system OCP2 with optimal cost $\mathcal{J}_*$, and let $S_{N,\gamma} \subset C[0,T] \oplus L_2[0,T]$ be the set of optimal solutions $(z_{N,\gamma}, u_{N,\gamma})$ of the problem $P_{N,\gamma}$ with optimal cost $\mathcal{J}_{N,\gamma}$. Then, $\{S_{N,\gamma}\}$ converge to S_* in the sense*

$$\lim_{\gamma \to \infty} \lim_{N \to \infty} d(S_{N,\gamma}, S_*) = 0 \,,$$

and $\{\mathcal{J}_{N,\gamma}\}$ converges to $\mathcal{J}_*$ in the sense

$$\lim_{\gamma \to \infty} \lim_{N \to \infty} \mathcal{J}_{N,\gamma} = \mathcal{J}_* \,.$$

Here, the measure d of $C[0,T] \oplus L_2[0,T]$ is defined as

$$d(X,Y) = \sup_{\{(z,u) \in X\}} \inf_{\{(\bar{z}, \bar{u}) \in Y\}} \left(\|z - \bar{z}\|_{C[0,T]} + \|u - \bar{u}\|_2 \right) \,,$$

for X, $Y \subset C[0,T] \oplus L_2[0,T]$.

In other words, Theorem 4.1 ensures that given a sequence of solutions $\left\{ (z_{N,\gamma_p}, u_{N,\gamma_p}) \in S_{N,\gamma_p} \right\}$ there exists a subsequence $\{(z_{N_k,\gamma_{p_l}}, u_{N_k,\gamma_{p_l}})\}_{k,l=1}^{\infty}$ and a solution $(z_*, u_*) \in S_*$ such that

$$\|u_{N_k,\gamma_{p_l}} - u_*\|_2 \longrightarrow 0$$
$$\|z_{N_k,\gamma_{p_l}} - z_*\|_{C[0,T]} \longrightarrow 0 \,,$$

as N_k, γ_{p_l} tend to infinity.

5   Simulations and experiments for the REEL II

In the simulations shown below obtained through the Basis Algorithm, we have used the nondimensional equations describing the motion of the robotic eel. Thus the axes on the plots are all unitless. The friction coefficients $\bar{\mu}^{\perp}$ and $\bar{\mu}^{\parallel}$ are set to 18 and 1.8, respectively. The non-dimensional inertial parameter $\bar{J}$ is taken to be 0.37. These values are taken to match experimental data taken in previous work [16]. The cost to optimize is

$$\mathcal{J} = \int_0^T \left(\dot{\phi}_1^2 + \dot{\phi}_2^2 + \dot{\phi}_4^2 + \dot{\phi}_5^2 \right) dt \,,$$

which corresponds to the energy expenditure of the joint actuators after time $T = 2\pi$. Also, for each input we consider the truncated basis

$$\frac{1}{\sqrt{\pi}}\sin(ft), \qquad \frac{1}{\sqrt{\pi}}\cos(ft), \quad 1 \le f \le 5.$$

In the following, we will compare some of the optimal gaits presented in [3] using this method with the open-loop gaits proposed in [16], some of which are motivated by biological observations [7]. In this and subsequent comparisons, the initial and final states for the optimal solutions are chosen to match those found in the corresponding traveling wave approach, so a direct comparison can be made.
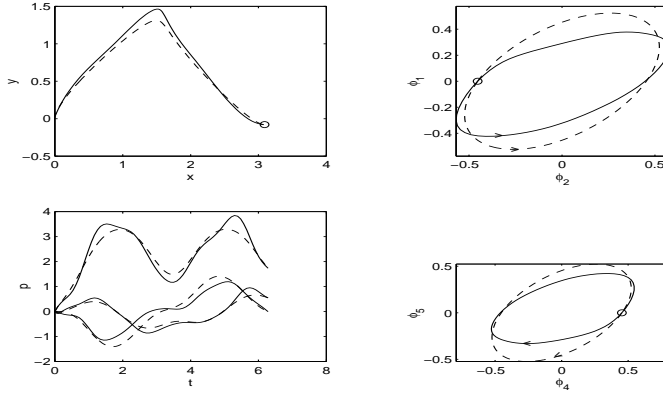
Figure 3: Comparison between a traveling wave (shown dashed) and the optimal approach (shown solid) of the forward motion of the eel building up momentum. The costs are $\mathcal{J} = 3.45$ and $\mathcal{J} = 2.9$, respectively.

Forward motion

The path described in Figure 3 by the eel to move forward by using a traveling wave and the optimal motion look quite similar. The optimal gait in the shape variables seems to be a kind of deformation of the traveling wave, just the one needed to generate almost the same time evolution in the forward momentum, p_1, and in the components, p_2 and p_3. It is interesting to note that the magnitudes of the joint angles ϕ_1 and ϕ_5 are quite smaller than in the traveling wave, whereas with the other two angles, ϕ_2 and ϕ_3, they are quite similar. Indeed, the optimal gait seems to be a traveling wave with smaller amplitudes in the head and tail of the eel. In relation to the other comparisons presented below, this comparison is the one that presents the smallest saving

of energy. This suggests that the traveling wave approach is actually very appropriate to drive the eel.
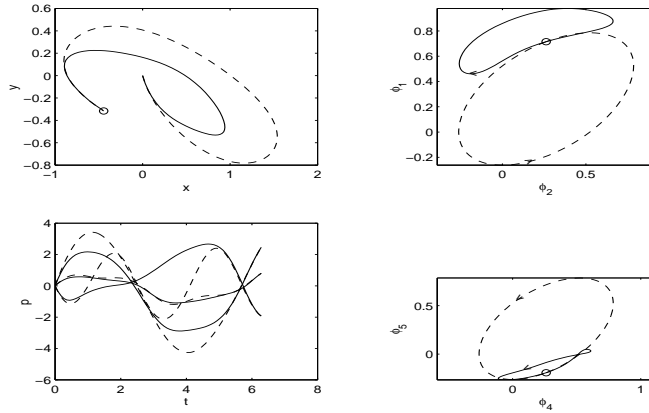
Figure 4: Comparison between a traveling wave (shown dashed) and the optimal approach (shown solid) of the turning in place motion of the eel. The costs are $\mathcal{J} = 3.443$ and $\mathcal{J} = 1.4414$, respectively

Turning motion

The gait in Figure 4 corresponds to a turning in place motion. Note that in this comparison the shape plots are quite different between the two gaits. The relative saving of energy is also quite large.
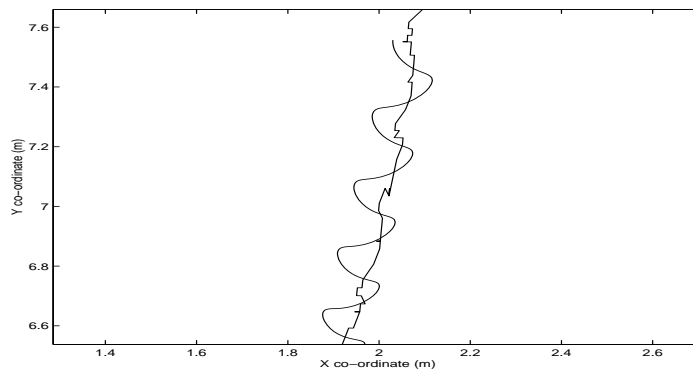
Figure 5: Matching of the optimal forward motion of Fig.5 with experimental data.

Comparison with experimental motion

In Figures 5 and 6, we show some comparisons of the motions obtained in the simulations and those implemented in the robotic eel whose experimental data was extracted with a video camera. The process of extracting data from video images captures the centroid and the orientation of the major axis of the body of the eel, so we do not expect an overlap of both curves. Generally, the simulation results, which show the position and orientation of the center of the mass of the middle link *only*, will generally fluctuate more, centered on the experimental data. In general this shows good agreement of the simulations with the experimental motions obtained in the real robot.
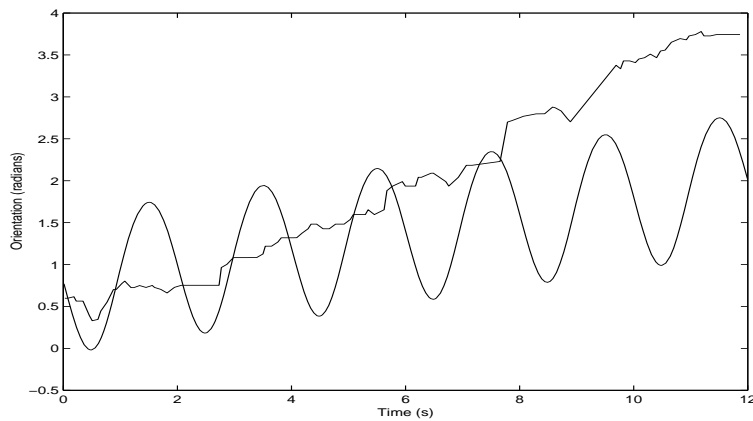
Figure 6: Matching of the optimal turning motion of Fig.6 with experimental data.

The only gait that showed a marked mismatch between experiment and simulation was the pure rotation gait, as shown in Figure 6. The rotation accomplished in the experiment turned out to be *larger* than predicted by the model. We attribute the gain in the experimental data to added mass effects of the water that we did not take into account in our model for the eel.

Acknowledgments

References

[1] A. Bloch, P.S. Krishnaprasad, J.E. Marsden and R.M. Murray, "Nonholonomic mechanical systems with symmetry", *Arch. Rational Mech. Anal.* **136** (1996) 21–99.

[2] G.S. Chirikjian, J.W. Burdick, "The kinematics of hyper-redundant locomotion", *IEEE Trans. Robot. Automat.* **11** (6) (1995) 781–793.

[3] J. Cortés, S. Martínez, J.P. Ostrowski and K.A. McIsaac, "Optimal gaits for dynamic robotic locomotion", *Int. J. Robotics Research* **20** (9) (2001) 707–728.

[4] O. Ekeberg, "A combined neuronal and mechanical model of fish swimming", *Bio. Cyber.* **69** (1993) 363–374.

[5] C. Fernandes, L. Gurvits and Z.X. Li, "Near-optimal nonholonomic motion planning for a system of coupled rigid bodies", *IEEE Trans. Automat. Control* **39** (3) (1994) 450–463.

[6] T. Fukuda, A. Kawamoto, F. Arai, H. Matsuura, "Steering mechanism of underwater micro mobile robot", *Proc. IEEE Int. Conf. Robot.&Automat.*, Nagoya, Japan, 1995, 363–368.

[7] S. Hirose, *Biologically Inspired Robots: Snake-like Locomotors and Manipulators*, Oxford University Press, Oxford, 1993.

[8] S.D. Kelly and R.M. Murray, "Geometric phases and robotic locomotion", *J. Robotic Systems* **12** (6) (1995) 417–431.

[9] S. Kobayashi, K. Nomizu, *Foundations of Differential Geometry*, Interscience Publishers, Wiley, New-York, 1963.

[10] J. Koiller, K. Ehlers and R. Montgomery, "Problems and progress in microswimming", *J. Nonlinear Sci.* **6** (1996) 507–541.

[11] V.R. Kumar and K.J. Waldron, "A review of research on walking vehicles". In O. Khatib, J.J. Craig and T. Lozano-Prez, eds. *The Robotics Review 1* (1989) 243–266. MIT Press.

[12] A.D. Lewis, J.P. Ostrowski, R.M. Murray and J.W. Burdick, "Nonholonomic mechanics and locomotion: The snakeboard example, *Proc. IEEE Int. Conf. Robot.&Automat.*, San Diego, 1994, 2391–2397.

[13] S. Martínez, *Geometric methods in nonlinear control theory with applications to robotic systems*, PhD Thesis, Universidad Carlos III de Madrid, 2002.

[14] J. Mason and J. W. Burdick, "Construction and modeling of a carangiform robotic fish". *Int. Symposium on Experimental Robotics*, Sydney, Australia, 1999.

[15] T. McGeer, "Passive dynamic walking". *Int. J. Robotics Research* **9** (2) (1990), 62–82.

[16] K.A. McIsaac, *A hierarchical approach to motion planning with applications to an underwater eel-like robot*, PhD Thesis, University of Pennsylvania, 2001.

[17] K.A. McIsaac and J.P. Ostrowski, "Motion planning for dynamic eel-like robots, *Proc. IEEE Int. Conf. Robotics&Automation*, San Francisco, 2000, 1695–1700.

[18] R. C. Michelson and S. Reece, "Update on flapping wing micro air vehicle research-ongoing work to develop a flapping wing, crawling entomopter". In *13th Bristol Intl. RPV/UAV Systems Conference Proceedings*, 30.1–30.12, Bristol England, March 1998.

[19] J.P. Ostrowski, *The Mechanics and Control of Undulatory Robotic Locomotion*, PhD Thesis, California Institute of Technology, Pasadena, 1995.

[20] J.P. Ostrowski and J.W. Burdick, "Controllability tests for mechanical systems with symmetries and constraints *J. Appl. Math. Comp. Sci.* **7** (2) (1997) 101–127.

[21] J.P. Ostrowski and J.W. Burdick, "The geometric mechanics of undulatory robotic locomotion", *Int. J. Robotics Research* **17** (7) (1998) 683–702.

[22] S. Smale, "Topology and Mechanics", *Inv. Math.* **10** (1970) 305–331.

[23] J. J. Videlos, *Fish Swimming*. Chapman and Hall, New York, 1993.